TARADCOM

R and D RESEARCH

TECHNICAL REPORT

NO. 12498

FORMATION AND FAILURE OF ELASTOMER NETWORKS VIA THERMAL, MECHANICAL AND SURFACE CHARACTERIZATION

CONTRACT NO. DAAK30-78-C-0098

DECEMBER, 1979

by DAVID W. DWIGHT & JAMES E. McGRATH
DEPARTMENT OF MATERIALS ENGINEERING
and DEPARTMENT OF CHEMISTY
VIRGINIA POLYTECHNIC INSTITUTE AND
STATE UNIVERSITY
BLACKSBURG, VIRGINIA 24060

U.S. ARMY TANK-AUTOMOTIVE
RESEARCH AND DEVELOPMENT COMMAND
Warren, Michigan 48090

(9) Final Technical Report, 24 Aug 78-30 Jun 80

SECURITY CLASSIFICATION OF THIS PAGE (When Data Entered)

REPORT DOCUMENTATION PAGE

READ INSTRUCTIONS BEFORE COMPLETING FORM

1. REPORT NUMBER

2. GOVT ACCESSION NO.

3. RECIPIENT'S CATALOG NUMBER

(6) 4. TITLE (and Subtitle)
Formation and Failure of Elastomer Networks via Thermal, Mechanical and Surface Characterization

5. TYPE OF REPORT & PERIOD COVERED
Final Technical Report
Aug. 24, 1978 - June 30, 1980

6. PERFORMING ORG. REPORT NUMBER

(10) 7. AUTHOR(s)
David W. Dwight and James E. McGrath

(15) 8. CONTRACT OR GRANT NUMBER(s)
DAAK30-78-C-0098

9. PERFORMING ORGANIZATION NAME AND ADDRESS
Department of Materials Engineering and Chemistry
Virginia Polytechnic Institute and State University
Blacksburg, VA 24061

10. PROGRAM ELEMENT, PROJECT, TASK AREA & WORK UNIT NUMBERS
CMS 612601.H 910011
(12) 61

(11) 11. CONTROLLING OFFICE NAME AND ADDRESS
U. S. Army Tank-Automotive Research and Development Command
Warren, MI 48090

12. REPORT DATE
December 1979

13. NUMBER OF PAGES
51

(18) 14. MONITORING AGENCY NAME & ADDRESS (if different from Controlling Office)
TARADCOM
(19) 12498

15. SECURITY CLASS. (of this report)
UNCLASSIFIED

15a. DECLASSIFICATION/DOWNGRADING SCHEDULE

16. DISTRIBUTION STATEMENT (of this Report)
Distribution Unlimited.

This document has been approved for public release and sale; its distribution is unlimited.

17. DISTRIBUTION STATEMENT (of the abstract entered in Block 20, if different from Report)

18. SUPPLEMENTARY NOTES

19. KEY WORDS (Continue on reverse side if necessary and identify by block number)

Fracture mechanism	TGA TMA
SBR Degradation	ZnO particles
ESCA	Oxidative embrittlement
SEM/EDAX	

20. ABSTRACT (Continue on reverse side if necessary and identify by block number)

This work focussed upon development of ESCA, SEM/EDAX, TGA, DSC and TMA methodologies for synthetic elastomer compounds typically used in tank track pad service by the U. S. Army. The initial goal was to develop a molecular model of the failure mechanisms that lead to costly pad replacement. Exploratory measurements were conducted on fully compounded, uncured rubber, and pre- and post-service track pads. Studied also were laboratory-prepared samples involving variable matrix (SBR, EPDM and 50/50 SBR/BR) as well as zinc oxide particle shape and size.

DD FORM 1 JAN 73 1473 EDITION OF 1 NOV 65 IS OBSOLETE

UNCLASSIFIED

SECURITY CLASSIFICATION OF THIS PAGE (When Data Entered)

80 7 28 058

20. The chemistry of elastomer cure and in-service degradation was monitored with ESCA. This analysis indicate that the sulfur content decreased in curing, and the oxygen content increased during service. Heterogeneities were discovered on failure surfaces: (1) clumps of ZnO particles, (2) aliphatic-rich layers and (3) high sulfur regions. These all could act as sites for crack initiation. No aggregation of ZnO was found in laboratory blends, independent of particle size and shape. SEM/EDAX was most valuable to confirm the conclusions from ESCA and to define the sub-microscopic aspects of the locus of failure. Two different types of crack propagation surfaces have been identified at the 1-10 μm level: (1) granular and (2) smooth; the latter seem to be associated with "cabbage-leaf" abrasive wear at the macroscopic level, while the former is characteristic of large chunk failure. Swelling experiments showed little change after service, but TGA revealed a significant increase in volatiles content. Both thermo- and mechano-oxidative degradation of the elastomer clearly were caused by service conditions. These observations lead to a model invoking oxidative embrittlement and mechanical commination of the matrix, combined with initiation of cracks at stress concentrations caused by material inhomogeneities, protrusions on the terrain, and compression and shear forces.

An initial data base has been accumulated with surface and thermo-mechanical analysis that could provide useful structure-property information for further research and development of engineering elastomers.

FINAL REPORT

FORMATION AND FAILURE OF ELASTOMER NETWORKS VIA THERMAL, MECHANICAL AND SURFACE CHARACTERIZATION

by

David W. Dwight and James E. McGrath

prepared for

Department of the Army
Contract DAAK30-78-C-0098

December, 1979

U.S. Army Tank-Automotive Research and Development Command
Warren, Michigan 48090
Mr. Jacob Patt

Department of Materials Engineering and
Department of Chemistry

Virginia Polytechnic Institute and State University
Blacksburg, Virginia 24060

ABSTRACT

This work focussed upon development of ESCA, SEM/EDAX, TGA, DSC and TMA methodologies for synthetic elastomer compounds typically used in tank track pad service by the U.S. Army. The initial goal was to develop a molecular model of the failure mechanisms that lead to costly pad replacement. Exploratory measurements were conducted on fully compounded, uncured rubber, and pre- and post-service track pads. Studied also were laboratory-prepared samples involving variable matrix (SBR, EPDM and 50/50 SBR/BR) as well as zinc oxide particle shape and size.

The chemistry of elastomer cure and in-service degradation was monitored with ESCA. This anlysis indicate that the sulfur content decreased in curing, and the oxygen content increased during service. Heterogeneities were discovered on failure surfaces: (1) clumps of ZnO particles, (2) aliphatic-rich layers and (3) high sulfur regions. These all could act as sites for crack initiation. No aggregation of ZnO was found in laboratory blends, independent of particle size and shape. SEM/EDAX was most valuable to confirm the conclusion from ESCA and to define the submicroscopic aspects of the locus of failure. Two different types of crack propagation surfaces have been identified at the 1-10 μm level: (1) granular and (2) smooth; the latter seem to be associated with "cabbage-leaf" abrasive wear at the macroscopic level, while the former is characteristic of large chunk failure. Swelling experiments showed little change after service, but TGA revealed a significant increase in volatiles content. Both thermo- and mechano-oxidative degradation of the elastomer clearly were caused by service conditions. These observations lead to a model invoking oxidative embrittlement and mechanical commination of the matrix, combined with initiation of cracks at stress concentrations caused by material inhomogeneities, protrusions on the terrain, and compression and shear forces.

An initial data base has been accumulated with surface and thermo-mechanical analysis that could provide useful structure-property information for further research and development of engineering elastomers.

ACKNOWLEDGMENTS

We are grateful to Mr. Jacob Patt for his patience and support of our new Polymer Materials and Interfaces Research Laboratory, and to the Department of the Army for promoting this important type of application of academic research facility to the study of practical problems. Also, thanks are due to Randall Schlesinger for the ESCA data, and to several Polymer Laboratory students for help with many of the other experiments.

Table of Contents

"Table of Contents, continued"

List of Tables

List of Figures

INTRODUCTION

Military tracked vehicles (e.g., tanks) and personnel carriers utilize rubber track pads for the purpose of vibration damping, noise reduction, and preventing unnecessary damage to the terrain including concrete, asphalt, and macadam roadways. The majority of the track pads used by the U.S. Army are the T142 and T130 types. The former is used on the M48 and M60 series tanks and the latter on the M113 personnel carrier.

The T142 type pad, appears as in Fiqure A.. They are approximately 11 inches long and 2 inches thick, and are adhesively bonded to a steel shoe. Mounting to the track is via a single 0.7 inch diameter stud which is integral with the shoe.

There are many criteria these pads must meet before they will be accepted by the Army. The current standard is Military Specification (Milspec), MIL-T-11891B, written in 1960.

Physical properties routinely tested include hardness, tear resistance, ultimate tensile strength, and (added in 1972 ammendment) ozone resistance. Also, tensile strength and elongation are tested before and after aging for 70 hours at 158°F. Acceptable values for these tests are given in the mil-spec. Actual test procedures required are those of Federal Test Method Standard No. 601.

A road test of the pads also is required under the mil-spec. After a break-in (on paved roads) of 15 miles at 10 mph, 15 miles at 15 mph, and 15 miles at 20 mph, the track pads then are tested for a distance and ave-

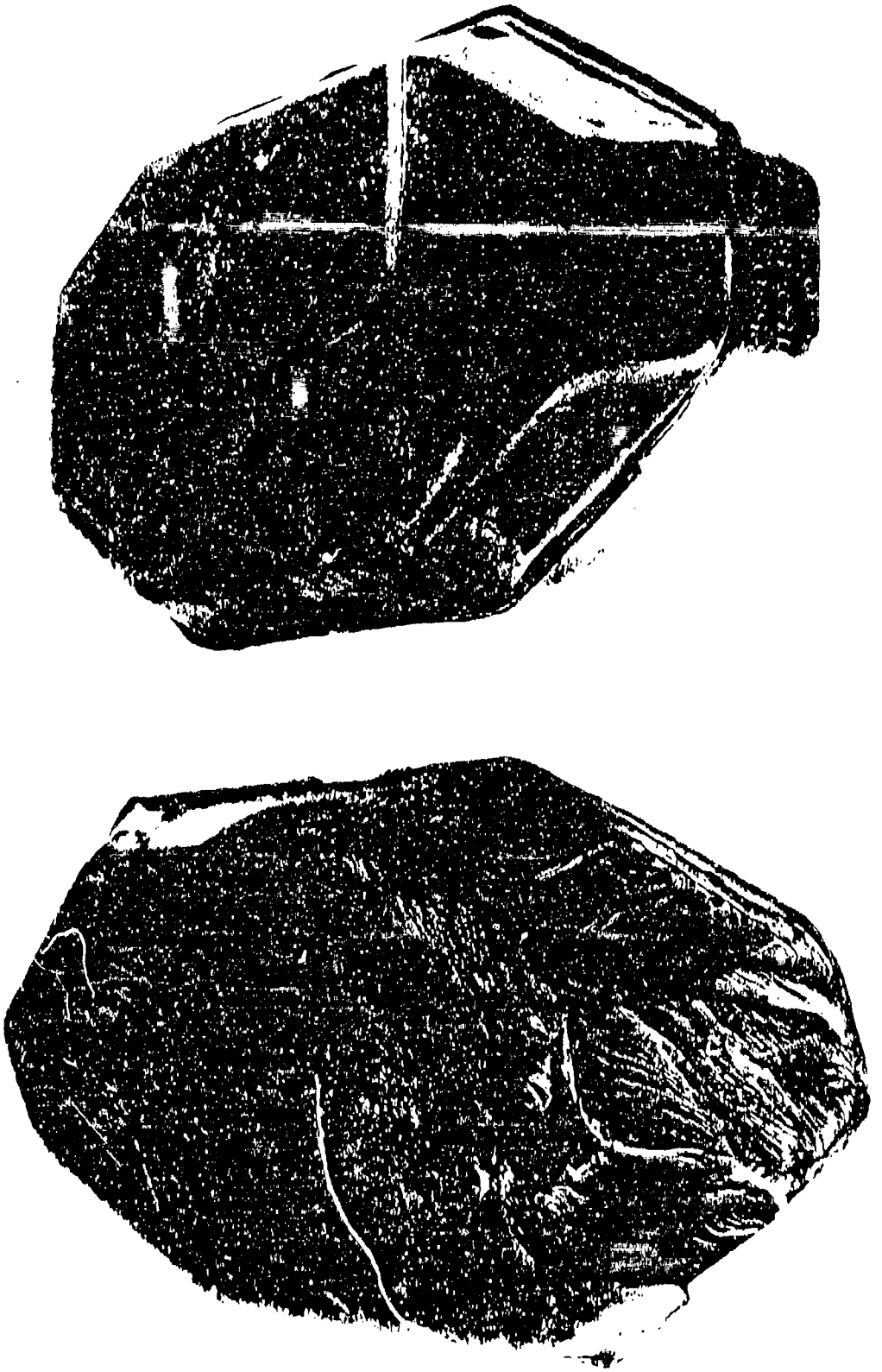

Figure 1. Photographs of T142 track pads. The top photo shows an unused example. A "chunk" type failure of the T142 is illustrated at the bottom. This is the most serious of the three most common failure modes because it occurred in less than 50 miles of service. The chunk that detached was roughly 1/5 the pad and a replacement pad was necessary.

rage speed determined by vehicle weight. For vehicles weighing 100,000 pounds or more (such as the M60 series tank) the distance is 1000 miles and the average speed 15 mph. At the conclusion of the road test, a visual inspection is made for blisters, cracks, and other defects.

Another requirement of the mil-spec is that the rubber portion of the track pad can be made entirely of synthetic rubber, i.e. no natural rubber. The material currently used by the track pad manufacturers is styrene-butadiene rubber (SBR). SBR has been the largest volume synthetic rubber in use for some time. However, it does not necessarily follow that it always should be chosen for current track pad applications.

The problem we are faced with is premature tank track pad failure, as illustrated in Figure 1B. Instead of lasting (ideally) 2000 miles, many pads fail in service after 200 miles or even less! TARADCOM has begun to focus on this problem via contract research to VPI & SU, and others. Thus far, Mr. Patt of TARADCOM has been submitting field service samples (e.g. good samples and failures). We have examined these samples by thermal, mechanical and surface characterization and are developing appropriate methodology to elucidate failure mechanisms which will ultimately result in the development of better elastomeric materials.

The samples we have investigated so far, are grouped in the following:

A. Uncured: This is an uncured version of the SBR used on the track pads. As compared with crosslinked rubber, these are soft and pliable.

B. Peel-treated: These samples were "peeled" from unused track pad and believed to represent the crosslinked network of SBR on the pads.

C. Failed: These samples are from track pads that failed in service. Pieces were taken from three different areas of pad, i.e. (a) leafy or layered, (b) pitted and (c) crumbly.

D. St. Joe Zinc Co.: Three additional samples of SBR material similar to that used in the track pads were supplied by the St. Joe Zinc Company. The three samples differed only in the size of the zinc oxide particles within the rubber. One contains fine spherical zinc oxide particles formed by an American process. The zinc oxide in the sample is very similar, but formed by a French process. The third one contains coarse acicular particles formed by an American process. These samples were solicited because experiments showed high concentration of ZnO on the fracture surfaces of field failure samples. These high concentrations were not formed on the other surfaces of the sample. This led us to suspect that ZnO might be involved in the premature failure of the track pads. This will be discussed in detail later.

E. N_2 Fracture Preservice track pads were immersed in liquid nitrogen and then fractured with a sharp blow from a sledge hammer. This is intended to collect samples from weaker areas or flow lines, which might be resembled to field fracture surfaces.

F. Goodrich: Two kinds of rubber, SBR and EPDM, were obtained from B. F. Goodrich Rubber Company. We intend to investigate the possibility of fracture improvement as we change from

SBR to EPDM.

Actual formulation of the St. Joe samples is as follows: SBR 1500 - 65%, N 330 Carbon Black - 29%, ZnO - 3%, Santocure NS - 1%, Stearic Acid - 1%, and Sulfur - 1%.

The types of experiments we have carried out are grouped in the areas to which they pertain as follows:

I. Structure-property Relations

A. Swelling

B. Tensile Testing

II. Thermal Properties

A. TGA

B. DTA

C. Accelerated Decomposition

III. Surface Analysis

A. SEM/EDAX fractography

B. ESCA surface chemistry

RESULTS

Swelling

Our first attempt at swelling experiments produced the results plotted in Figure 2. These results are not necessarily representative because there was not sufficient time (2 1/2 hours) to reach equilibrium. The rapid initial swell of the failed sample could be possible due to elastically stored mechanical energy in the rubber network. Plots of the result of our second swelling experiment, conducted over a period of 55 hours, which probably allowed enough time to reach equilibrium, are also shown in Figure 2. The lack of materials prevented use of the uncured and peel tested samples in our second swelling experiment.

The comparison between the St. Joe and the service failure swelling data suggests that crosslink density per se in the failed pads were not significantly different. Additional work is needed to explain the premature failure.

Tensile Testing

Four standard dogbones of each material were tested in the Instron machine at a crosshead speed of 4 inches per minute, either as received or after heating 5 minutes or 10 minutes at 325°C. The dogbones which were tested "as received" showed tensile behavior, ultimate stress and maximum elongation, very similar to those recorded in the TARADCOM report. The St. Joe materials correlated with the track pads.

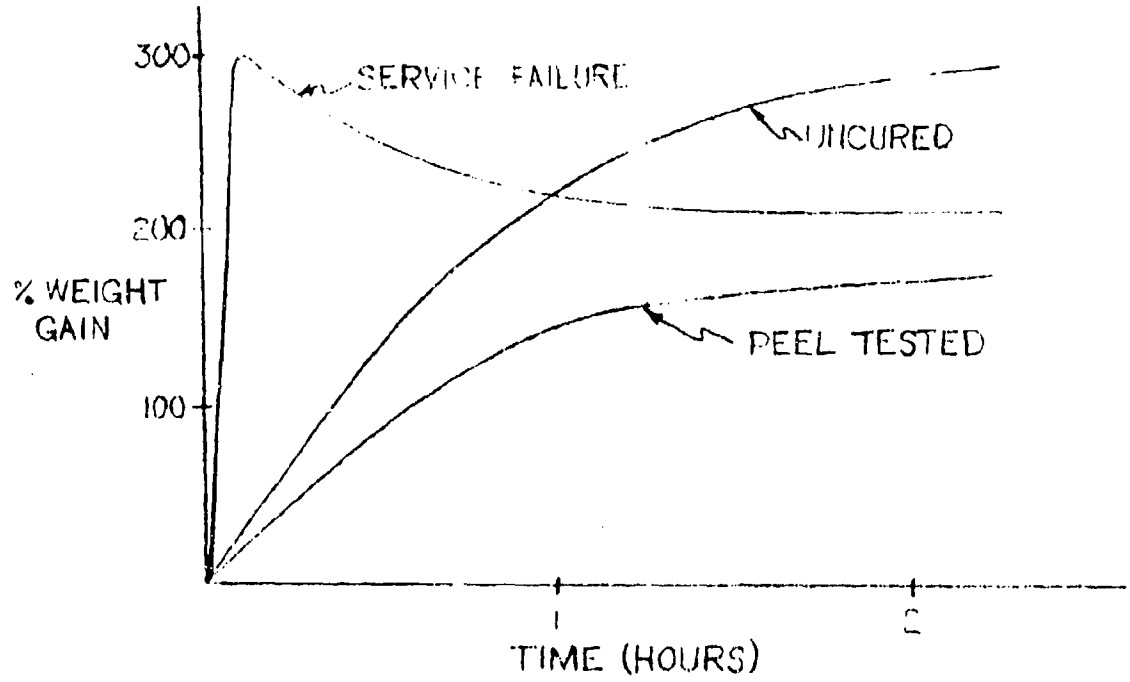

FIG. 2a FIRST SWELL EXPT.

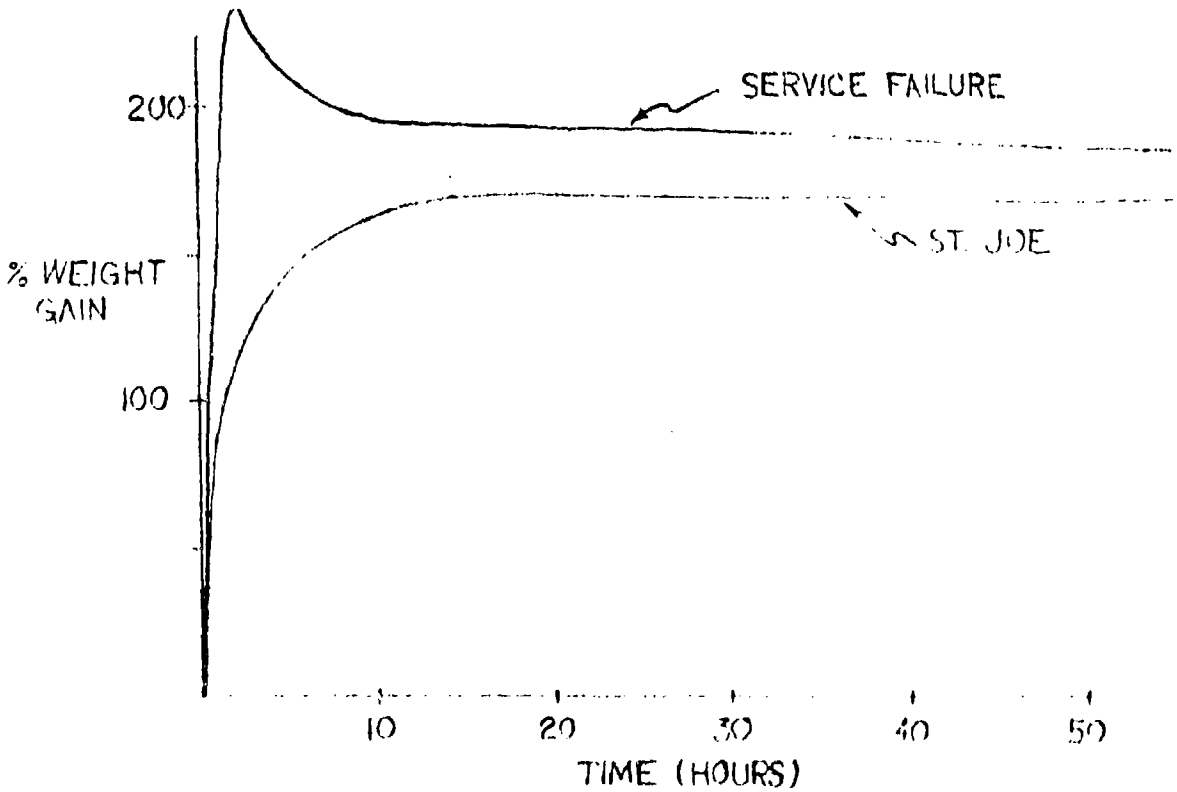

FIG. 2b SECOND SWELL EXPT.

0 min. "as received"		5 min. @ 325°C*		10 min. @ 325°C	
stress (ult.)	% elong. (max.)	stress	% elong.	stress	% elong.
4100 psi	430 %	1020	182	510	83
4220 psi	455 %	1270	235	530	86
4070 psi	440 %	1210	231	530	83

(all data $\pm$ 8%)

*This relatively high temperature was initially examined as an approach to accelerated degradation testing. Clearly, polydiene elastomer networks begin to degrade at much lower temperatures.

Progressive degradation is evident from the data gathered. The 5 and 10 minute degraded materials show higher initial strengths (at low strain) due possibly to oxidation of the rubber and consequent decrease in elasticity (slightly more brittle but stronger).

Fractographs of the fracture surfaces show no resemblance to the failed track pad fracture surfaces, zinc-oxide particles are not to be found on the dogbone surfaces. The fact that particles were found on the failed specimen surfaces quite possibly indicates that the rubber in the track pads may not have been blended properly (layers of ZnO particles provide a surface for failure).

TGA

Initial studies showed that ten percent weight loss occurred at approximately 370°C for the service failure material, and at approximately 440°C for the peel tested and St. Joe materials. These temperatures will be very dependent on the heating rate and atmosphere etc.. Much more research is needed and is in progress. However, the service failure materials do show weight loss at lower temperatures which undoubtedly reflects a degradation process different from the new materials (See Figure 18).

Degradation of the St. Joe materials at 440°C is attributed to pyrolysis of the rubber. Degradation at 325°C corresponds to the first marked weight loss of the St. Joe rubber, at the somewhat rapid heating rate of 40°K per minute. Slower heating rates and isothermal degradation studies should be more revealing.

DTA (or DSC)

In differential thermal analysis, heat flow (evolution or absorption) is measured as a function of temperature. The transitions observed in Figure 19 can be interpreted as exotherms due to oxidation of the rubber. Such reaction exotherms can show correlations to the TGA weight loss. A combination of DTA (DSC) and TGA gives a very useful thermal fingerprint of the test specimens which can be used to develop laboratory accelerated degradation tests.

SEM

EDAX detected Al, Cl, Si, K, Ca, Fe, and Zn in the bulk and in the particles on the surface. The needle-like particles shown in fractographs are confirmed by ESCA and EDAX to be zinc oxide as was suspected. The agglomeration of ZnO particles on the failure surfaces could certainly be involved in the premature failure of the track pads. These layers appear to be primarily "aliphatic" material derived from the polydiene component of the SBR. The presence of the ZnO particles suggest that the blending of the rubber with the compounding ingredients, is inadequate. More intensive mixing with longer time cycles are suggested.

Fracture surfaces derived from tensile test specimen showed no ZnO particles on the fracture surfaces of the controlled St. Joe materials. On the other hand, the ZnO particles were observed on the surfaces of the failed pads. It would be of interest to observe whether inhomogeneities

could be created in the control materials by reducing the blending time. If this was feasible, additional degradation and tensile tests etc. could be conducted and might be revealing.

The granular appearance of fractographs is believed to be significant and probably results via the combined degradative action of stress, oxygen and heat. Further measurements of swelling and thermal analysis (DSC, TGA, and TMA) should further elucidate these observations.

ESCA

ESCA detected C, O, S, N, Zn, Cl, and Si on the failure surface of track pad materials. Carbon, oxygen, nitrogen, zinc and sulfur can be accounted for as constituents of the rubber and its curatives. The zinc was shown by EDAX to be ZnO, a curing agent. A post service failure ESCA run showed an increase in the ratio of oxygen to carbon by a factor of 4. This clearly reflects the oxidative degradation that is occuring, especially at the surface. Oxygen can, of course more easily diffuse and react at the surface. Even the control surface show some limited amount of oxidation. The failure surfaces are primarily "aliphatic" in nature which is presumably derived from the polydiene component of the SBR.

SEM and ESCA examination of (a) peel tested and (b) service failure samples (obtained by Dr. Dwight during a June 19, 1978 visit to TARADCOM) showed indications that deleterious inhomogeneities were present in the tract pads as manufactured. Fracture surfaces showed aggregates of ZnO particles and no aromatic (styrene) character was observed on laminar failures compared to the bulk, as determined by ESCA.

St. Joe Zinc Co. supplied three samples to elucidate the effects of ZnO size and shape.

Swelling experiments and TGA showed that the St. Joe formulations were very similar in network structure to the TARADCOM peel tested sample, as expected. However, significant thermo-oxidative degradation was indicated by the TGA result on the Service Failed sample and confirmed by the 4X increase in O/C ratio determined ESCA.

Each of the St. Joe samples was failed in tension, before and after exposure to 325°C for 5 and 10 minutes, and about 75% and 90% drop in stress-strain properties was noted. However, SEM examinations of all fracture surfaces never showed ZnO_2 even in the case of high aspect-ratio, acicular particles. Presumably this reflected very good mixing, which should be emulated by the commercial elastomer systems.

Chunky fracture surfaces of degraded rubber were observed at progressively higher magnification and underscore the effects of mechano-chemical and thermo-oxidative degradation: Micron-sized granular structures are created, and cracks propagate easily through this type of matrix.

Our tentative conclusions based on the above results are: (1) Large-scale batch blending as currently conducted probably does not produce a uniform, homogenious track pad, (2) Inhomogeneities such as ZnO can form aggregates which produces relatively weak regions and (3) Service conditions, which includes mechanical, thermal and oxidative degradation, further weakening the rubber. Improvements may be possible via improved stabilization approaches (e.g. more and better antioxidants), although new elastomeric materials (e.g. rather than SBR) may also be necessary to reflect the current use conditions for tank pads.

Optical microscopy has also been used to study the fracture surface of one failed pad. By comparison with the earlier specimens, it is clear

that different failure mechanisms are important, depending upon the time to failure. The short-life, chunk-failure now under investigation show brittle, cleavage propagation over most of the failure surface. A few small craters at the interface between the pad and metal backing plate appear to be the site of the failure initiation.

The figures 3-5 are three successive enlargements of the areas of concern. Small "craters" at the boundary between the metal bracket and the pad appear to be the locus for crack initiation. Cracks then appear to propagate in a brittle mode into the bulk of the pad, resulting in a "chunk failure". Scanning Electron Microscopy of the craters show small bubbles and cracks. We feel this indicates a localized rapid degradation of explosive proportions occurred here. The combined pressures from the service condition and micro-decomposition embrittle the rubber matrix, providing easy crack propagation. SEM photo-micrographs of areas A and B were similar. Both areas have a multitude of microscopic cracks characteristic of track pad fracture surfaces observed previously. It appears that degradation via crosslinking had transformed the rubber to a granular structure in which many cracks are growing. We chose an intact side of this track pad as a control. Even in this case, where the material looked "like new" to the eye, microscopic degradation prevailed at the surface giving micrographs with the appearance of "mud-cracking".

We used one of the track pads supplied that had not been run in service (Goodyear label). To try to draw out possible heterogeneities without tank-type service, we first froze the intire pad and shoe in liquid nitrogen and separated the pad from the metal track shoe. Incidentally, separation appeared to occur at the metal surface because rust formed uniformly on the surface immediately, whereas if adhesive had been left on the shoe surface, then rusting would have been prevented or delayed.

Figure 3

Figure 4

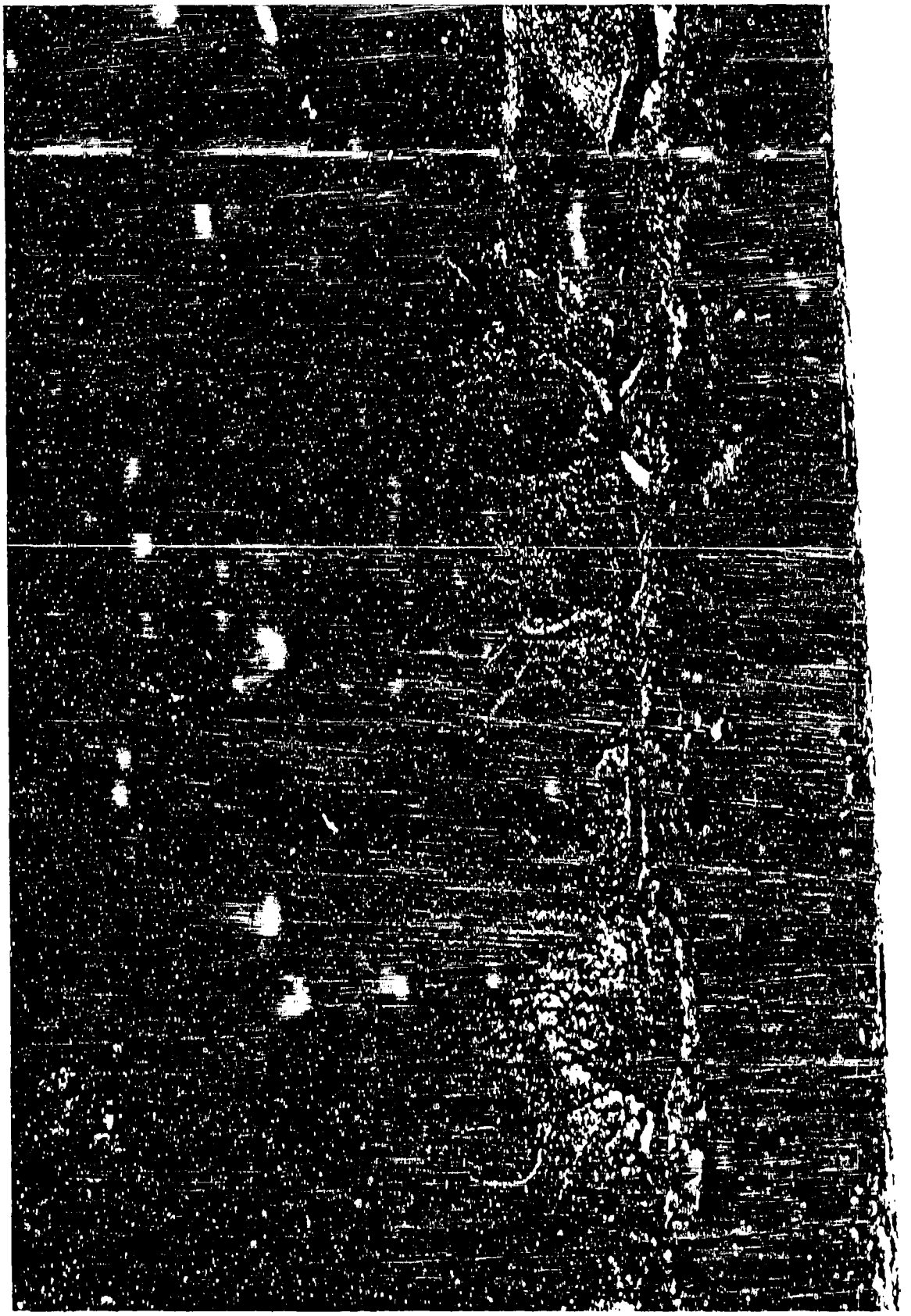

Figure 5

Subsequently, we froze the rubber pad in liquid nitrogen and then fractured it with a sharp blow from a sledge hammer. Indeed, the pad fragmented in a peculiar pattern that gave the appearance of being weaker areas of "flow lines" from processing. For example "weld-like" phenomena are sometimes observed during injection molding.

We have completed SEM/EDAX of five different regions taken from the liquid nitrogen fractured pad. However, no unusual features were observed (ie. zinc oxide particle concentrations) either physically or chemically in field-service failures.

We investigated the possibility of utilizing the thermal mechanical analysis (TMA) attachment of the thermal analysis unit to probe uncured, cured, and tested elastomeric tank pad test specimen. TMA had the advantage of being rapid and employing rather small quantities of material.

Moreover, it is possible to use penetration, thermal coefficient of expansion, or extension type measurements. One might expect that compounding nonuniformity, differing degrees of cure and oxidative stress induced degradation could be investigated by this technique. This experiment produces data that are approximately proportional to a modulus-temperature plot.

Our initial studies examined penetration vs. temperature for uncured SBR and EPDM. Cured Goodyear and Firestone SBR pads, chunk failures in pads run less than fifty miles and various long-run failure specimens. The glass transition could be easily detected and was relatively invariant (-31 to -42°C). Measurement of Tg by this method may well be 10 - 15°C higher than lower frequency tests such as the torsion pendulum or rheovibron.

As expected, the uncured SBR and EPDM was totally penetrated (90-100%)

at 75°C. The cured and aged samples were anticipated to be penetrated much less. This was observed, but thus far the data are too scattered to establish a trend. Further studies, especially with higher loads, will be conducted. The extensional mode will also be examined.

SUMMARY

1. The objective of this research was to develop methods to characterize the effect of chemical and physical phenomena occuring during track pad failures. Exploratory measurements by a variety of Surface Analysis and Thermo-Mechanical Analysis techniques have been conducted.
2. Methodology was developed to obtain meaningful results on track pads, both "as received" and after service failure.
3. Control data from standards were collected as a base of comparison for (a) molecular structure of elastomer and (b) ZnO particle size and shape.
4. Several specimens from each of three classes of sample types were analyzed: (a) uncured, (b) cured and (c) service failed.
5. ESCA was successfully applied to follow the cure and degradation of elastomers. This constitutes the first appearance of this type study in the literature.
6. Failure mechanisms were classified and preliminary models of molecular-level mechanisms involved in each type were developed.
7. The separate roles of materials and process variables were defined and partially clarified.
8. An initial data base has been accumulated upon which to expand the application of surface and thermomechanical analysis to research and development problems at TARADCOM.

CONCLUSIONS

1. ESCA is very useful to monitor the chemistry of elastomer cure and service degradation.
2. SEM/EDAX is a valuable tool for defining the submicroscopic physical aspects of elastomer failure: the locus of fracture initiation and propagation.
3. The combination of the above techniques provide data that permit an initial understanding of molecular-level mechanisms important to the formation and failure of elastomer networks.
4. Three different types of failures have been identified: (a) chunking, (b) leaf and (c) granular.
5. Unexpected heterogeneities were discovered, indicated: (a) clumps of ZnO particles, (b) thin, "aliphatic" rich polydiene derived surface layers and (c) high sulfur and silica filler regions. These could all act as sites for crack initiation.
6. Thermo-oxidative degradation of the elastomer can be detected that clearly is caused by service conditions. This serves to embrittle the matrix via excessive crosslinking, thus rendering crack propagation easier.
7. Continued in depth studies are required to (a) obtain statistically significant information on failure mechanisms, (b) establish precision and accuracy of measurements, (c) establish generality of application and (d) explore thermo-mechanical techniques that could provide useful structure property information.

APPENDIX 1

SCANNING ELECTRON MICROSCOPY (SEM)

-AND-

ENERGY DISPERSIVE ANALYSIS OF X-RAYS (EDAX)

SEM

A versatile tool such as the scanning electron microscope (SEM) has many material characterization capabilities. For our particular problem the SEM was used along with attachments to take fractographs (photographs of fractured surfaces) and to do an energy dispersive analysis of X-rays (EDAX).

The principle of the SEM is illustrated schematically in Fig. 5. Electrons from a filament are accelerated by a voltage and directed down the center of an electron optical column consisting of two or three magnetic lenses. These lenses cause a fine electron beam to be focused onto the specimen surface. Scanning coils placed before the final lenses control the rastering of the electron beam across the sample surface. The same circuit which controls the scanning coils in a cathode ray tube (CRT). As a result, the position of the electron beam on the sample in the SEM and on the CRT display are synchronized.

The electron beam incident on the specimen surface caused various phenomena, of which the emission of secondary electrons is the most commonly used to form high resolution images. The secondary electrons strike a detector and the resulting current is amplified and used to modulate the brightness of the CRT. Consequently, an image of the surface is progressively built up on the screen. Because of the great depth of field of the SEM, the image produced is of dramatic three dimensional quality and promotes fractographic analysis.

Since the SEM has no imaging lenses, any signal that arises from the action of the incident electron beam (reflected electrons, transmitted electrons, emitted light, X-rays, etc.) can be used to form an image on the CRT screen. In a different type of mode, the X-rays emitted from the

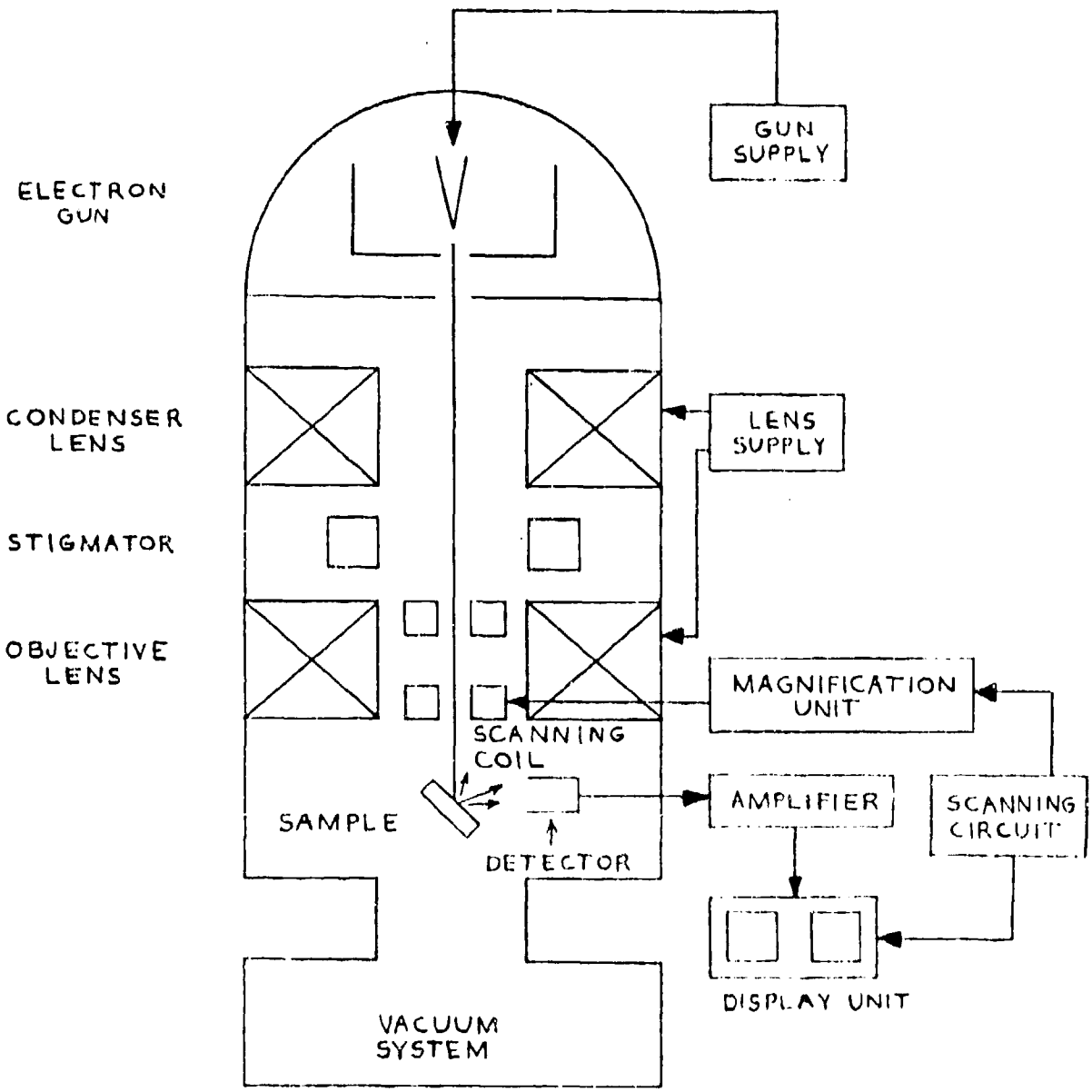

FIG. 6 SIMPLIFIED BLOCK DIAGRAM OF SCANNING ELECTRON MICROSCOPE

sample are used to provide information about the nature and amount of elements present in the material. This type of analysis can be used on the surface or in the bulk material, depending on the energy of the incident electron beam. In this method, known as energy dispersive analysis of X-rays, the photon is converted into an electric pulse which is proportional to the energy of the X-ray. This pulse is amplified, converted to a voltage pulse, and fed into a multichannel analyzer. The analyzer sorts out the pulses according to their energy and stores them in the memory of the correct channel. The resulting spectrum can be displayed on a CRT, plotted on a chart, or printed our numerically. From this, the elements present can be determined since the individual energies of the X-rays emitted are characteristic of the different elements.

SEM's

Figure No.	Description
7	Zinc oxide particles - peel test sample
8	Zinc oxide particles - field service failure
9	Granular failure surface showing increasing magnification of crack tip region
10	Top - "Mud cracked" appearance of pad surface that looks perfect by eye
	Bottom - More granular field failures
11	St. Joe Zinc Company "model" specimens tensile failure surfaces
	Top - after 300°C for 10 minutes
	Bottom - as received (cured)
	Note differences in these surfaces compared to field failure surfaces
12	"Cabbage-leaf" type field failure, series of increasing magnifications

Figure 7


50 µm

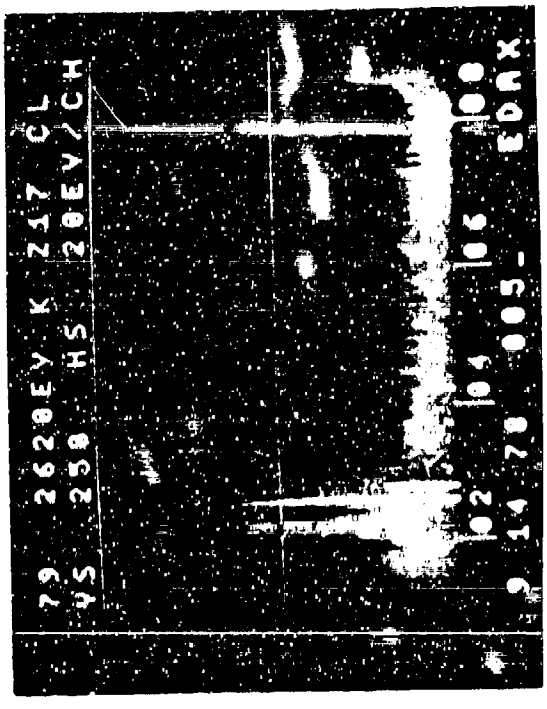
79 2620EY K 217 CL
4S 230 HS 20EV/CH
02 04 06 08
14 28 005- EDAX

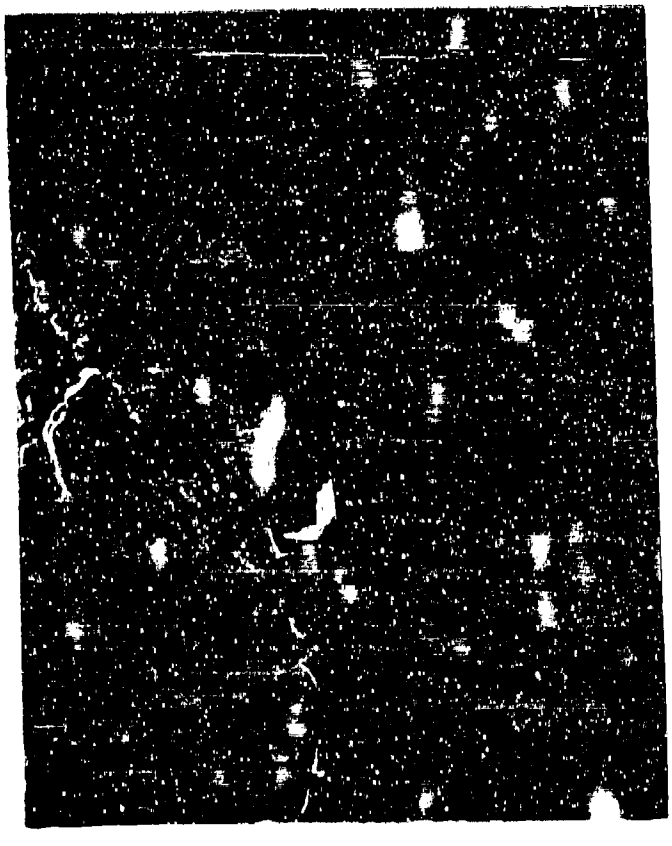

Figure 8

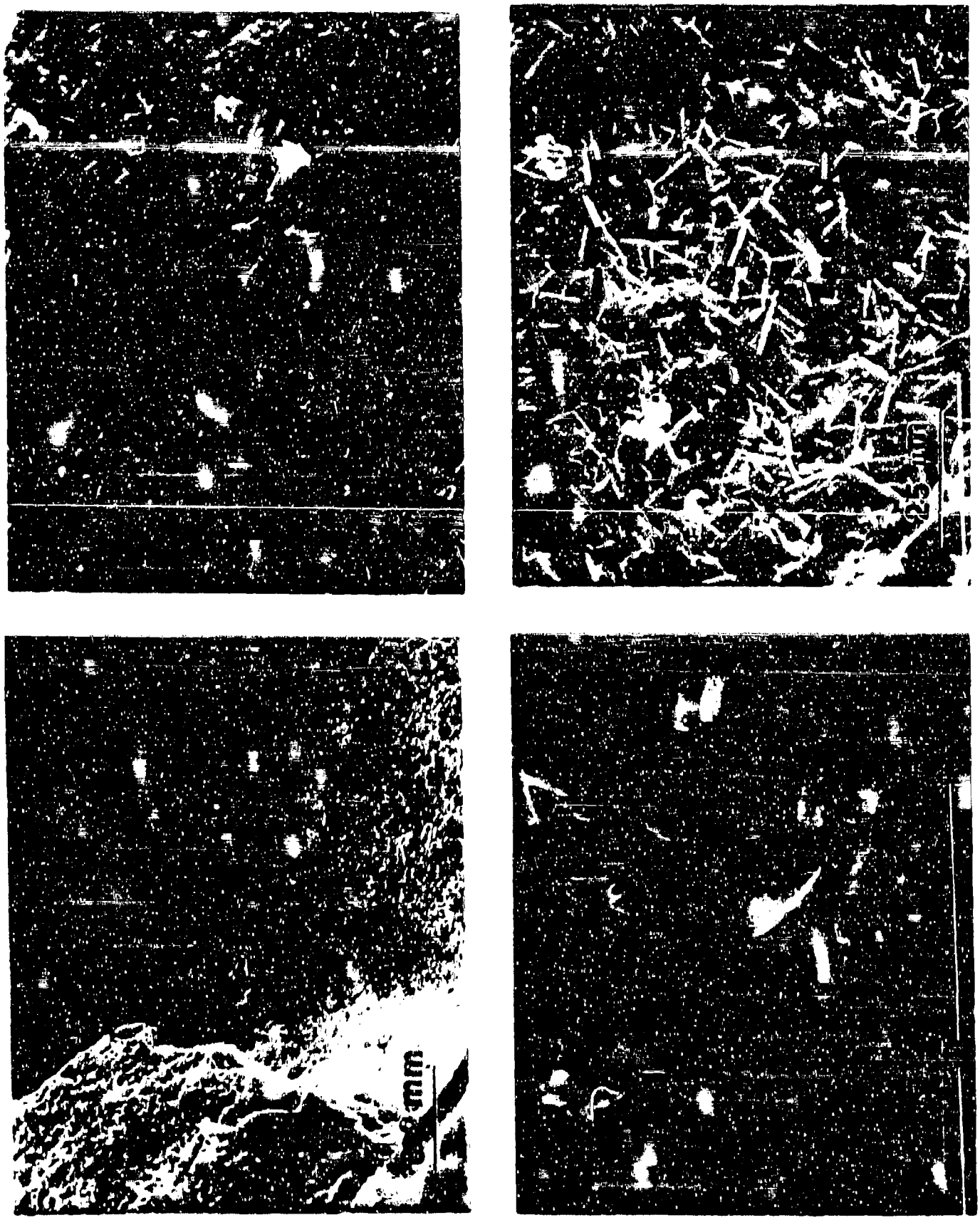

Figure 9

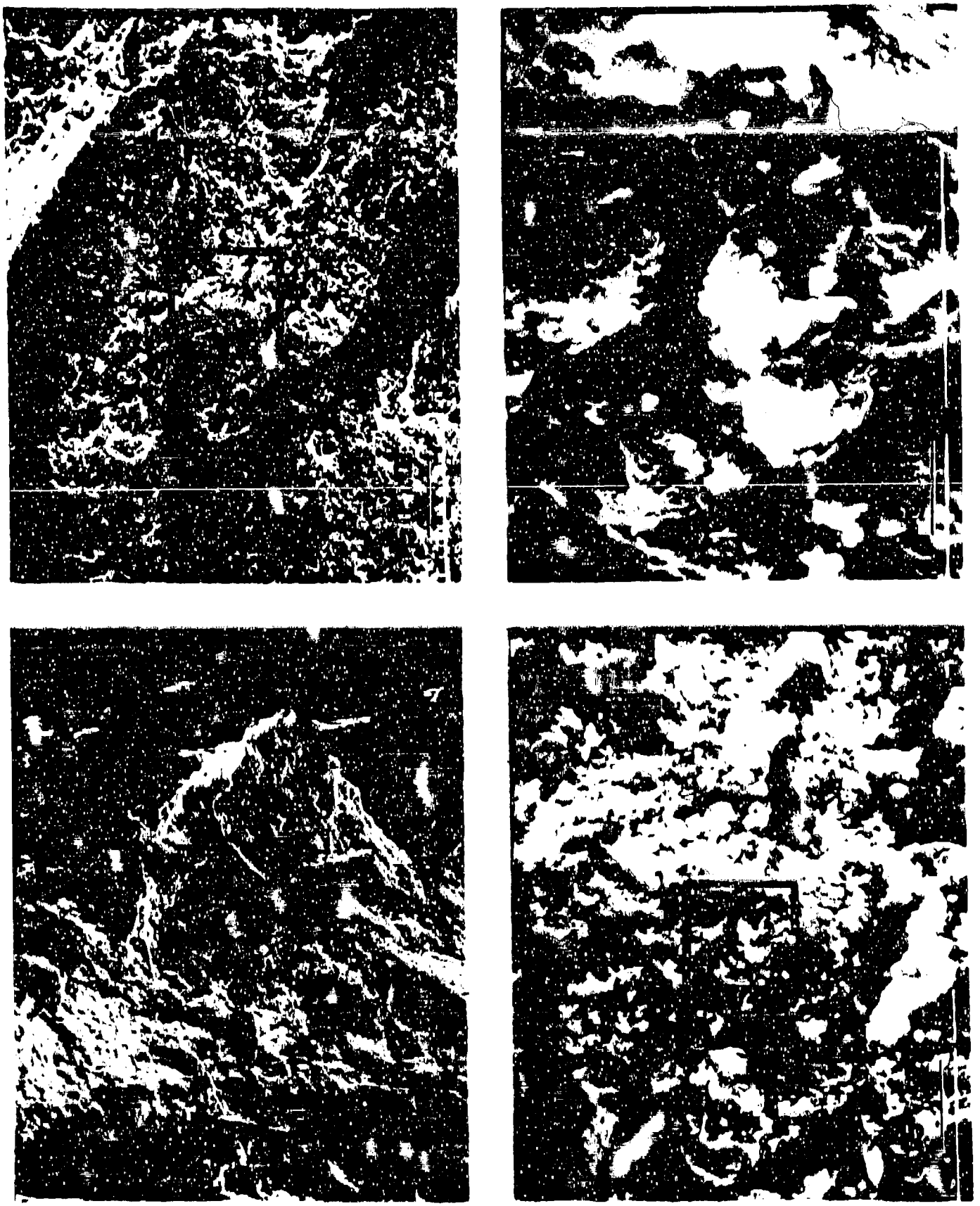

Figure 10

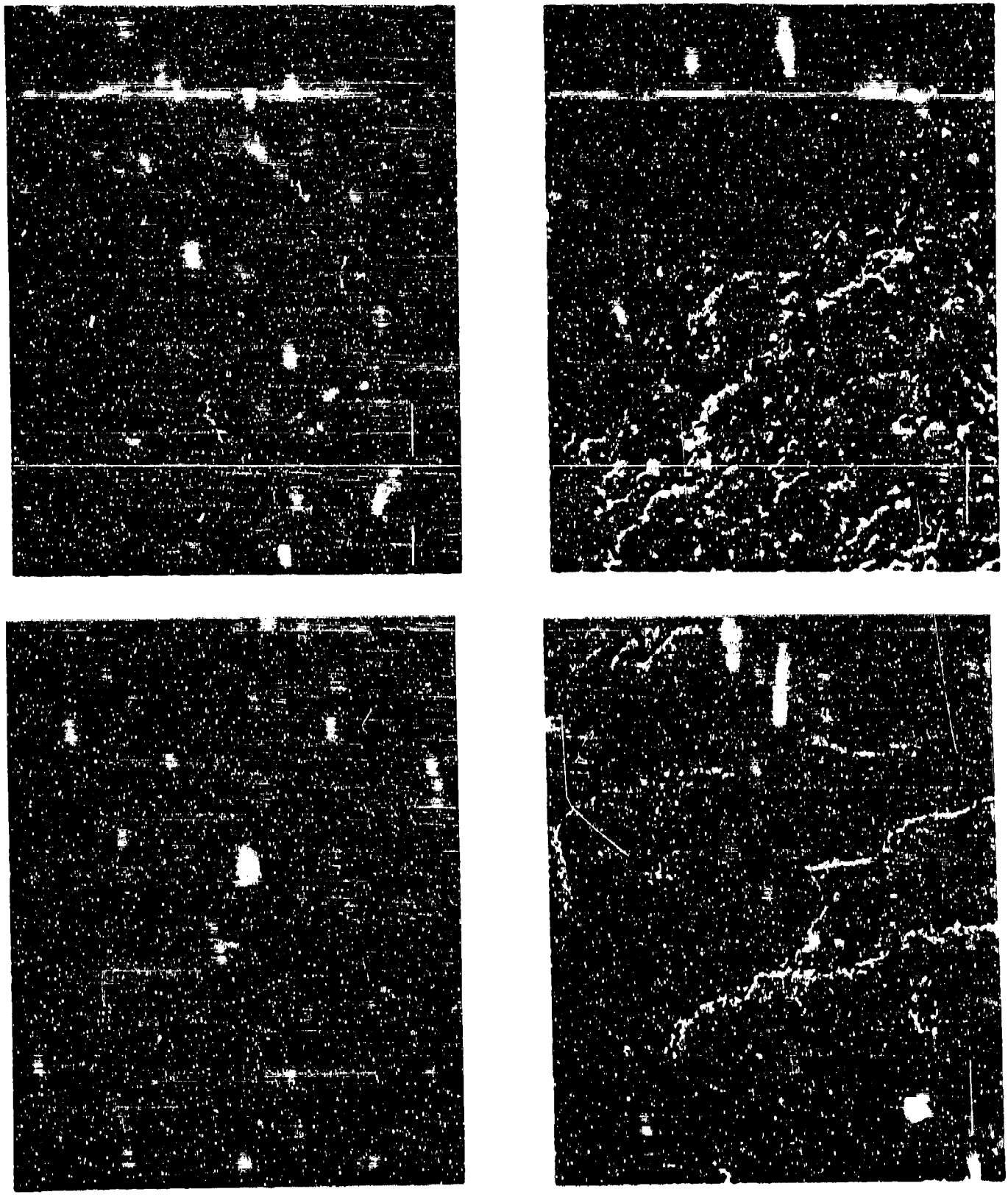

Figure 11

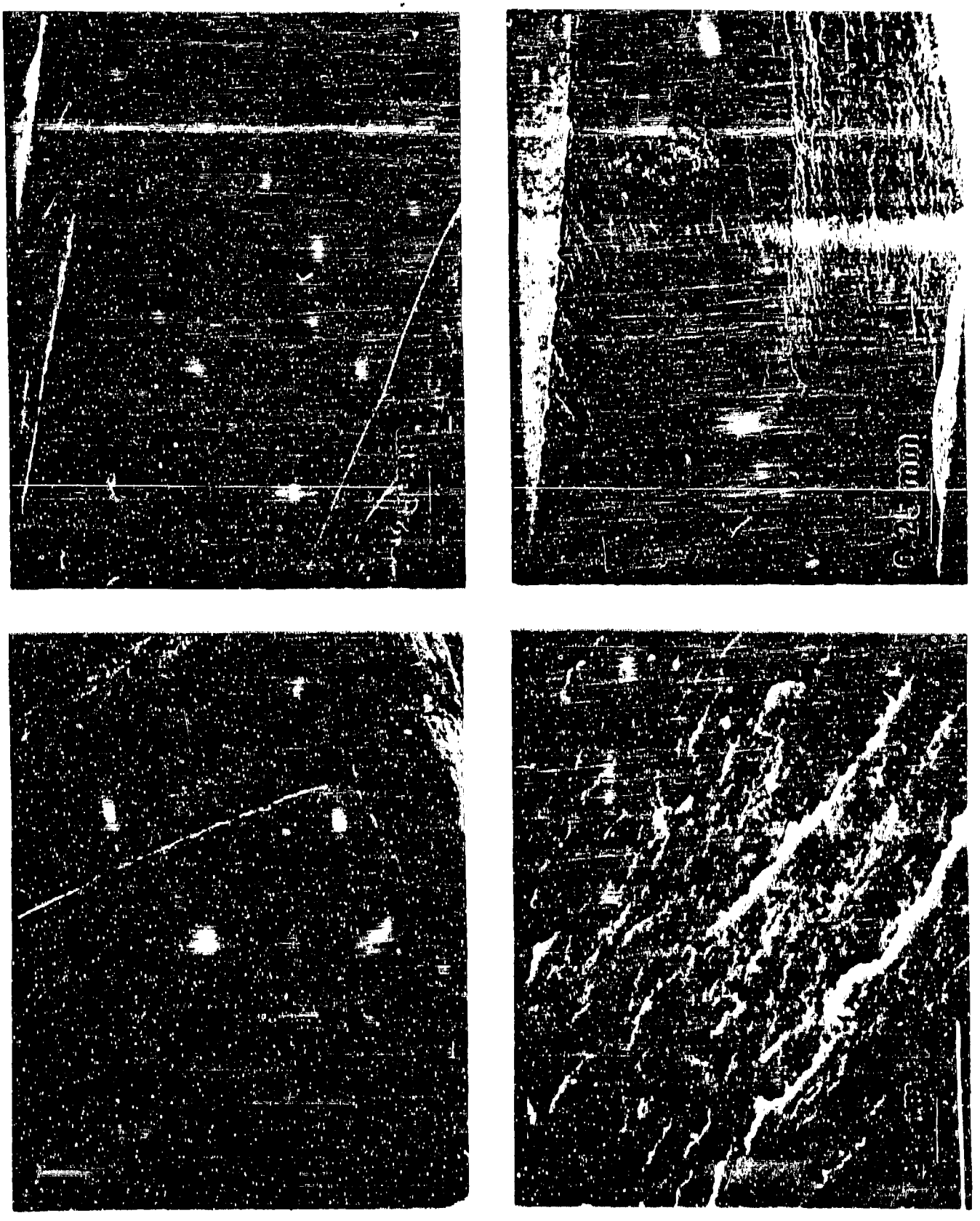

Figure 12

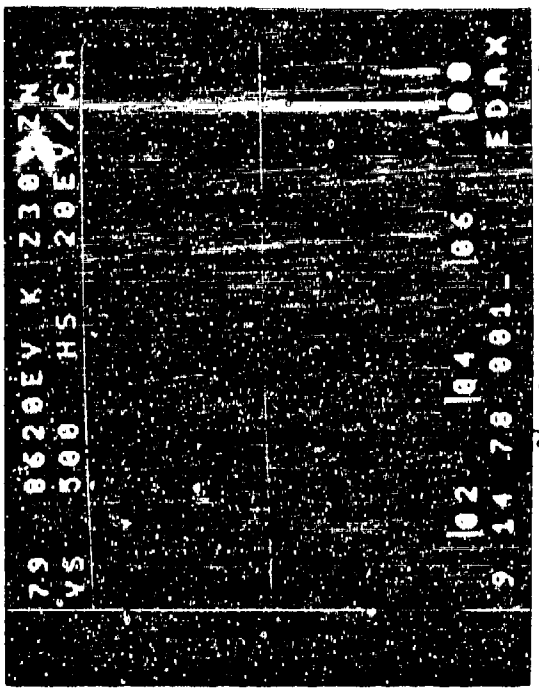
79 8620EV K 230 2N
YS 500 HS 205 A/CH
9 14 78 001 106 100
102 104 EDAX

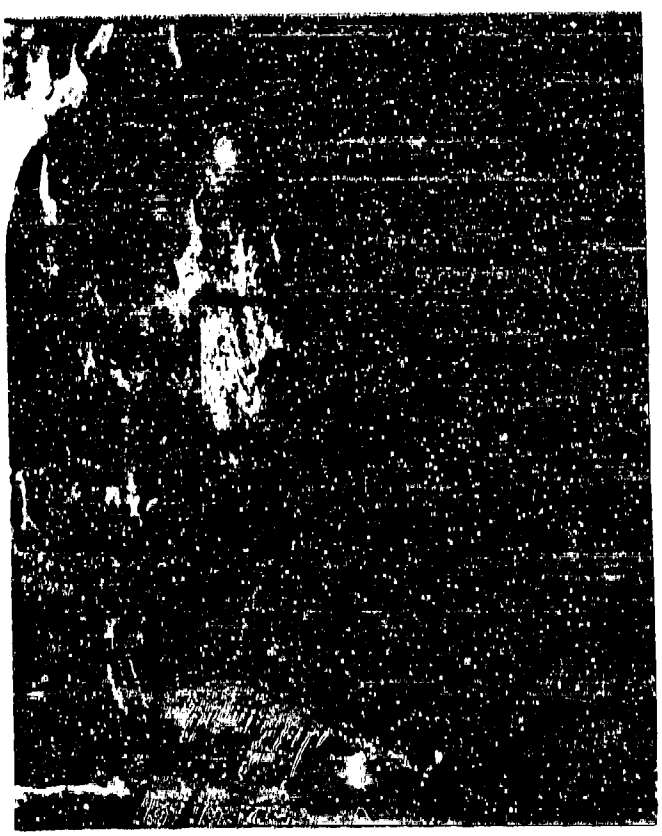

APPENDIX 2

X-RAY PHOTOELECTRON SPECTROSCOPY (XPS)

OR

ELECTRON SPECTROSCOPY FOR CHEMICAL ANALYSIS (ESCA)

ESCA

One of the most ideally suited techniques used to investigate the chemical nature of surfaces is Electron Spectroscopy for Chemical Analysis (ESCA). The instrument employed is composed of five basic components: (1) source, (2) sample compartment, (3) electron energy analyzer, (4)detector, and (5) readout system. The source produces an X-ray beam which is directed into the sample compartment where it impinges upon the material to be studied, causing the ejection of electrons as illustrated in Fig. 13a. The electron energy analyzer sorts the resulting electrons according to their kinetic energies (KE) and focuses them on a detector at the output. The detector produces an electrical signal proportional to the intensity of the emitted photoelectrons from the specimen and the readout system translates it into graphic form. From the kinetic energy and the energy in the X-ray beam ($h\nu$), the binding of an electron can be calculated by the relationship $E_b(e^-) = h\nu - KE$. The binding energy is characteristic of the element from which the electron is ejected. The quantity of electrons detected for each different KE value is proportional to the concentration of the element.

Moreover, changes in the chemical environment of an atom in a molecule produce chemical shifts in binding energy. These shifts reflect changes in chemical bonding or oxidation states and may be used to follow such changes on the surface as shown in Fig. 13b.

ESCA analyses were performed on cross-sections of the bulk on each of the track pads and also on three uncured compositions. The latter specimens were obtained independently from commercial sources.

The uncured samples all had higher oxygen and sulfur concentrations than any TARADCOM samples. It was encouraging to observe shake-up satellites in the SBR, but not in EPDM; thus our ESCA technique can distinguish

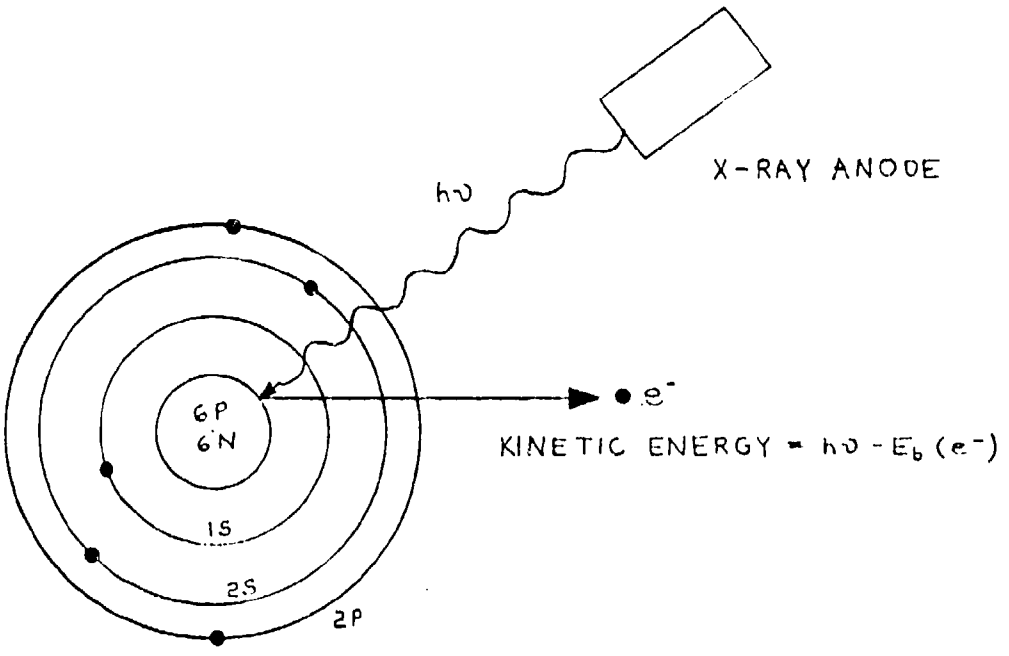

FIG. 13a CARBON 1S X-RAY PHOTOELECTRON PRODUCTION

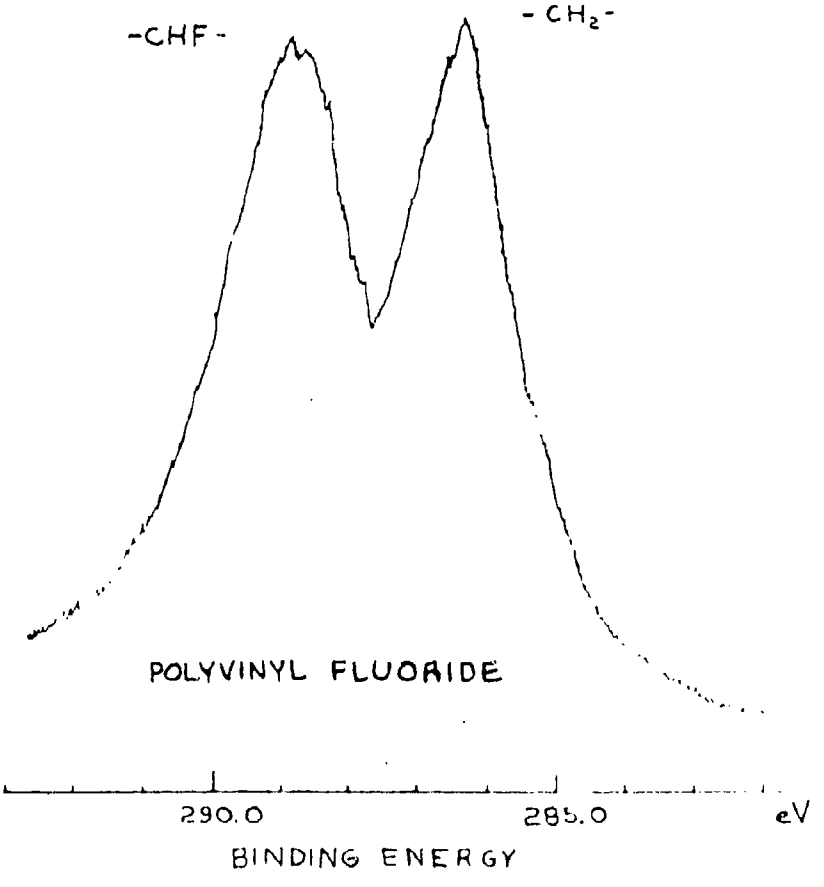

FIG. 13b CARBON 1S ESCA SPECTRUM ILLUSTRATING CHEMICAL SHIFT

between aromatic- and aliphatic- containing rubbers in these control samples.

Two of the six track pads recently received from TARADCOM had high oxygen concentrations, and they were also the only ones that had seen service. This apparent thermomechanical oxidation was seen in the first samples, too. All bulk cross-sections of track pads showed aromatic character (shake-up satellites).

ESCA analysis of the fracture regions show increasing amounts of oxygen and C-O bonds, and the absence of any aromatic (styrene) character. Certainly oxidative degradation in service is indicated. We are unable to determine whether the styrene component was thermolyzed in service or was absent from these regions as manufactured.

The quantitative analysis of the ESCA spectra that we have collected on track pad compositions, ranging from uncured to cross-linked to field tested to failure are listed in Tables 1-4.

The first eight entries in Table 1 were cut from various field tested track pads stocked at TARADCOM. The last five samples in Table 1 were taken from the pads sent in November 1978. Oxidative degradation is indicated by the oxygen concentrations, ranging from 3 - 12%. Sulfur on the other hand was detected only on one sample, and is 1% in that case.

Table 2 lists the ESCA results from six cured ("as received") track pads before field testing or service. Oxygen ranges lower, between 1 and 6%, and shake-up satellites (indicative of the styrene component) are usually apparent. Also, sulfur was normally detected at a bit less than 1%.

Four uncured compositions were studied and the results are listed in Table 3. Sulfur concentrations are significantly larger, ranging from 1 to 5%. Oxygen content was also higher than expected. Only in the 100% SBR was a shake-up satellite apparent in the carbon region.

In summary, sulfur concentration decreases upon vulcanization; its oxidation state is low and unchanged. Oxygen also decreases during cure. After track pad service, oxygen content increases and failure surfaces show high-energy carbon peaks from carbon-oxygen bonding. The aromatic component is absent from failure surfaces. These results provide an initial data base for ESCA analysis of rubber track pad compositions. Although the full significance of the data is yet to be determined through continued experiments, we have shown that ESCA is a valuable tool to follow the chemistry of vulcanization and thermo-oxidative aging in those elastomers.

ESCA analyses on five different samples taken from separate regions of one of the unused Goodyear track pads are summarized in Table 4; evidence for considerable chemical heterogeniety is clear. High oxygen concentrations occur at both rubber/metal and air interfaces. At the interface with the metal shoe, the radically different composition probably reflects the presence of adhesive. (Control samples of these adhesives would help clarify this analysis.) A significant amount of oxidized sulfur (169eV, sulfates) was found in the middle of the track pad, as well as the crosslink sulfur (163.5eV). There were very small or non-existent shake up satellites on the fracture surfaces. It is tempting to conclude that failure under stress in track pads tend to propagate through regions of inhomogeneous composition. In general, these regions show anomalously high concentrations of oxygen, zinc or sulfur, and low concentrations of styrene rubber component.

SUMMARY

ELECTRON SPECTROSCOPY FOR CHEMICAL ANALYSIS (ESCA)

I. SURFACE CONSTITUENTS DETECTED

* C, O, S, N, Zn, Cl, Si

II. POST SERVICE FAILURE

A. RATIO O/C INCREASES 4X

B. ALIPHATIC ON SURFACE

AROMATIC IN BULK

III. CONTROLS

A. FOLLOW CURE & SERVICE CHEMISTRY

B. DEFINE PAD UNIFORMITY

ENERGY DISPERSIVE ANALYSIS OF X-RAYS (EDAX IN SEM)

I. BULK CONSTITUENTS DETECTED

* Al, Si, Cl, K, Ca, Fe, Zn

II. SURFACE PARTICLES

* ZnO

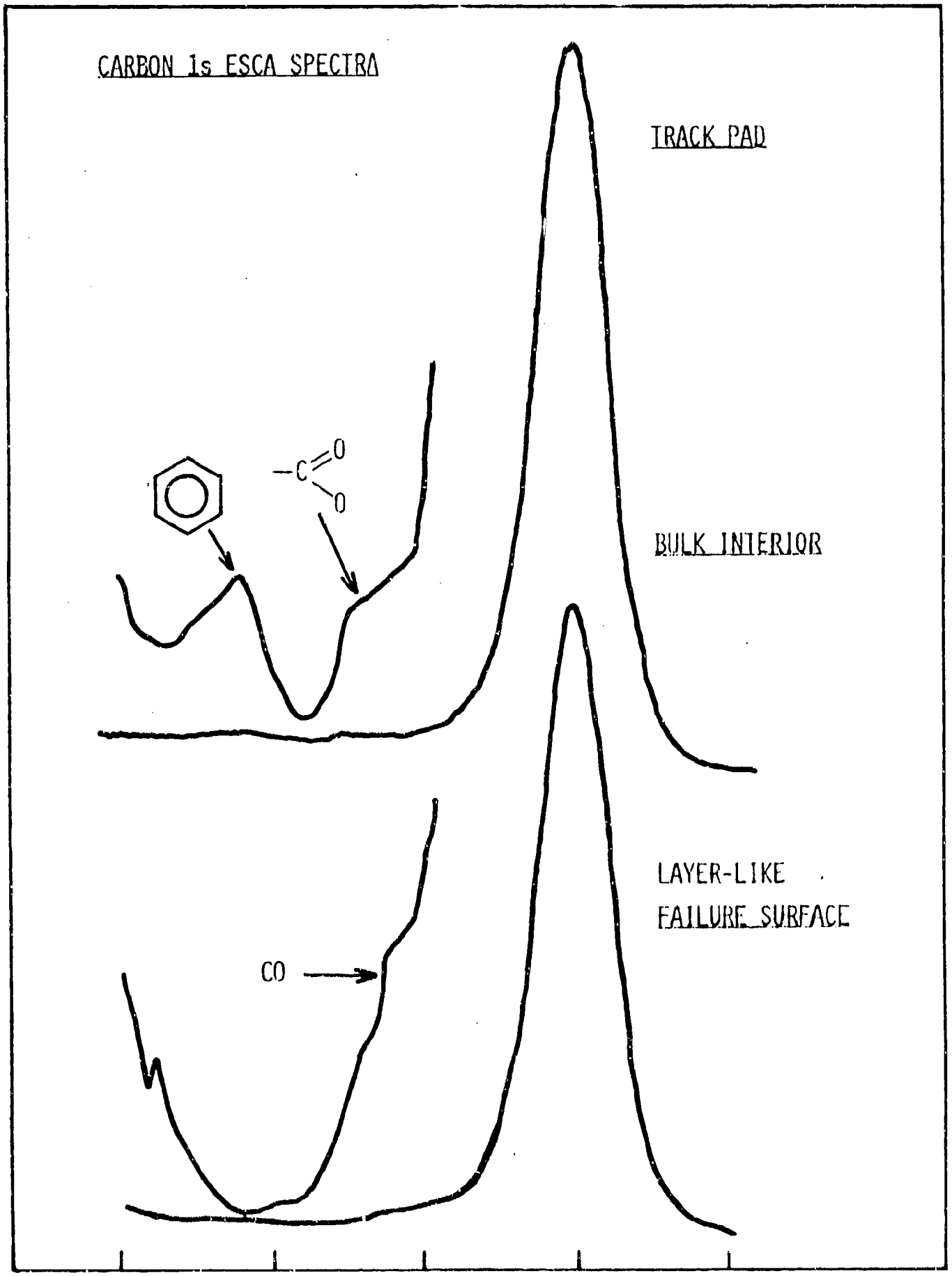
CARBON 1s ESCA SPECTRA
TRACK PAD
BULK INTERIOR
LAYER-LIKE
FAILURE SURFACE
-C=O
O
CO
294
291
288
285
282

Figure 14

Table 1 Failure Surfaces
TARADCOM FIELD PADS
ESCA Peak Assignments, Binding Energies (eV) and Concentrations in Atom Percent

Sample	C (3) (291.6±.4)	C (2) (288.7±.6)	C (1) (285.0)	O (532.4±.4)	N (399.8±.3)	S (163.6±.3)	Si (102.4±.3)	Cl (199.2±.1)	Zn (89.6±.4)
DWD 1-28-3	—	—	90.0	8.1	0.9	—	1.0	—	—
" inside	—	—	95.0	3.9	0.4	—	0.7	—	—
" outside	—	—	93.9	4.4	1.0	—	0.3	—	0.4
" inside	—	—	93.8	4.5	0.6	0.8	0.4	—	—
" outside	—	—	72.8	11.5	2.7	—	1.5	0.6	—
" middle	2.7	—	94.2	4.3	0.5	—	—	—	—
" layered	—	—	96.8	2.6	0.4	—	0.2	—	—
" layered	—	—	95.9	3.3	0.5	—	0.4	—	—
DWD 1-31-5 Firestone	—	6.4	81.9	10.3	1.0	—	0.5	—	—
DWD 1-31-6 Firestone	0.6	2.9	90.0	4.4	0.5	0.9	0.2	—	0.4
DWD 1-31-6 Crater	—	3.9	87.2	6.8	1.8	—	0.4	—	—
Ribbed Middle	—	—	95.6	7.0	1.4	—	—	—	—
Outside Rough	—	—	94.6	3.3	1.6	—	0.5	—	—

Table 2 Cured Rubber (untested)
TARADCOM PADS AS RECEIVED
ESCA Peak Assignments, Binding Energies (eV) and Concentrations in Atom Percent

Sample	C (3) (291.6±.4)	C (2) (288.7±.6)	C (1) (285.0)	O (532.4±.4)	N (399.8±.3)	S (163.6±.3)	Si (102.4±.3)	Cl (199.2±.1)	Zn (89.6±.4)
Peel Tested DWD 1-28-2	—	—	98.0	1.4	—	0.6	—	—	—
DWD 1-31-1 Goodyear	—	—	91.2	5.9	0.9	0.6	0.6	0.3	0.4
DWD 1-31-2 Goodyear	1.1	—	94.2	2.7	0.6	0.7	0.3	—	0.3
DWD 1-31-3 Goodyear	0.9	—	93.7	3.3	0.7	1.0	0.4	—	—
DWD 1-31-4 Goodyear	2.8	—	93.2	2.0	0.6	0.9	0.2	—	0.3
DWD 1-31-5 Firestone	0.8	—	94.3	2.8	0.8	0.8	—	—	0.5

Table 3 Uncured Rubbers
ESCA Peak Assignments, Binding Energies (eV) and Concentrations in Atom Percent

Sample	C (3) (291.6±.4)	C (2) (288.7±.6)	C (1) (285.0)	O (532.4±.4)	N (399.8±.3)	S (163.6±.3)	Si (102.4±.3)	Cl (199.2±.1)	Zn (89.6±.4)
Army Uncured DWD 1-28-1	—	—	95.8	1.3	0.6	2.2	—	—	0.2
DWD 1-32-3 50SBR/50BR	—	8.0	80.3	10.1	0.5	1.0	—	—	—
DWD 1-32-2 EPDM	—	2.7	87.0	4.5	0.4	5.0	0.4	—	—
DWD 1-32-1 SBR	0.6	—	92.5	4.3	0.1	2.2	0.1	—	0.2

TABLE 4: ESCA PEAK ASSIGNMENTS, BINDING ENERGIES (eV) AND CONCENTRATIONS IN ATOM PERCENT

ıple	C (2) (288.7±0.3)	C (1) (285.0±0.0)	O (532.5±0.4)	N (399.8±0.1)	Si (102.5±0.2)	Cl (199.4±0.5)	Zn (89.2±0.0)	S (1) (168.9±0.5)	S (2) (163.4±0.6)
As Received	—	91	5.0	0.9	0.6	0.3	0.4	—	0.6
Liquid Nitrogen Fracture									
A. ∿ 1cm from metal backing	7	82	7.8	—	1.5	0.5	—	—	1.3
B. Metal-rubber interface	—	78	15.6	2.0	—	5.0	—	—	—
C. ∿ 3cm from metal backing	7	83	6.5	1.0	1.3	0.5	0.2	0.3	0.5
D. Razor blade cut ∿ 3cm from metal backing	6	85	6.0	1.0	0.8	0.4	—	0.3	0.4
E. Air-rubber interface	6	82	9.8	1.0	1.2	0.3	—	—	—

APPENDIX 3

THERMAL AND MECHANICAL ANALYSIS

Swelling

A swelling experiment is designed to determine the relative % crosslinks of different samples on a comparative basis. This can be done since the % weight gain is inversely proportional to % crosslinks in the material. Also, with a few calculations the average molecular weight between crosslinks can be determined. However, the quantitative aspects are well known to be not well resolved in filled elastomers.

The procedure for carrying our a swelling experiment by the gravimetric technique is given as follows. Specimens weighing approximately 2 gm each are cut from the samples to be tested and are placed in a stoppered flask containing enough swelling solvent, such as toluene, to cover the specimens. Periodically the specimens are removed, blotted dry with filter paper, and rapidly weighed. (The work should be carried our rapidly to avoid loss of solvent by deswelling and evaporation, causing the sample weight to drift downward.) This should be repeated until the samples reach their equilibrium degree of swelling (2-3 days). When equilbrium is reached, the final constant weight can be used to determine the % weight gain and the average molecular weight between crosslinks (M_x) from the following equations.

$$\% \text{ weight gain} = \frac{w_s - w_o}{w_o} \times 100$$

$$\% \text{ weight gain} \propto \frac{1}{\#\text{ crosslinks}}$$

equilibrium volume after swelling $$V_s = \frac{w_o}{p_2} + \frac{w_s - w_o}{p_1}$$

equilbrium concentration of the polymer $$c = \frac{V_s w_o}{p_2}$$

average molecular weight between crosslinks $M_x = \frac{-V_1 p_2 (c^{1/3} - c/2)}{(\ln(1-c) + c X_1 c^2)}$

where w_s = swollen wt.

w_o = original wt.

p_1 = density of solvent

p_2 = density of polymer

V_1 = molar volume of the solvent

X_1 = polymer-solvent interaction parameter

Tensile Testing

Because many polymers are widely used for their mechanical properties, some measure of these characteristics is essential. Tensile testing provides one with much of this kind of information. A tensile testing machine, such as the Instron, is required.

In short, a dogbone sample is held between two clamps and is pulled apart at a constant rate until the sample breaks. (The pulling rate is known as the rate of strain and can be varied to suit the material being tested.) Since the upper clamp contains a load cell, the force developed is measured continuously as the sample is elongated. This information is recorded as a force versus elongation plot. From measuring the original cross sectional area and the original length of the sample, a stress versus strain plot, can be made. Stress-strain curves serve to define the modulus, yield stress and elongation at break, and other pertinent information used in characterizing the material.

After pulling the sample apart, the two fracture surfaces can be kept to make fractographs or used for a chemical analysis of its surface.

TGA

Thermogravimetric analysis (TGA) is a dynamic technique in which the

FIG. 15 STRESS vs. STRAIN DATA

SAMPLE 30-1

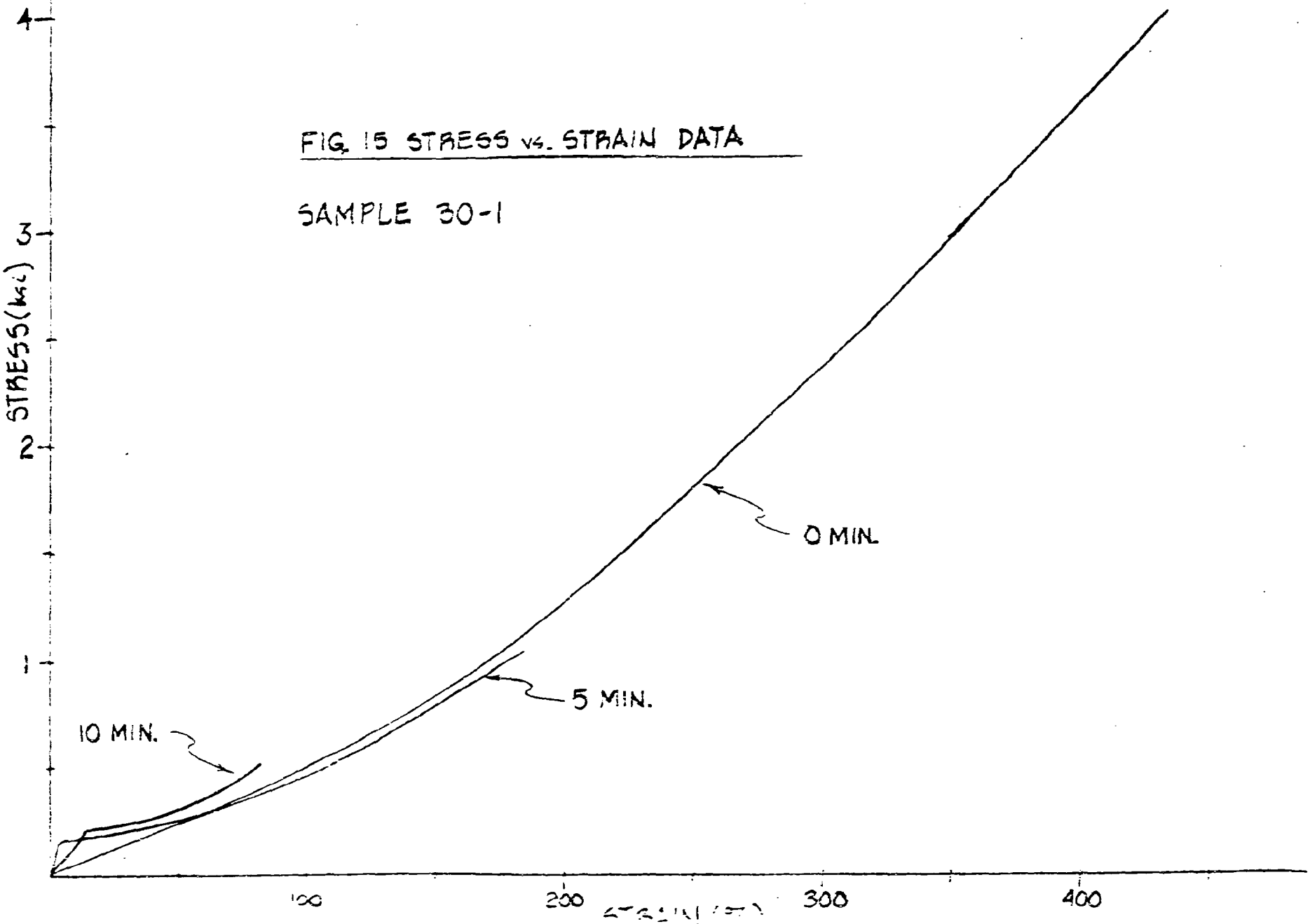

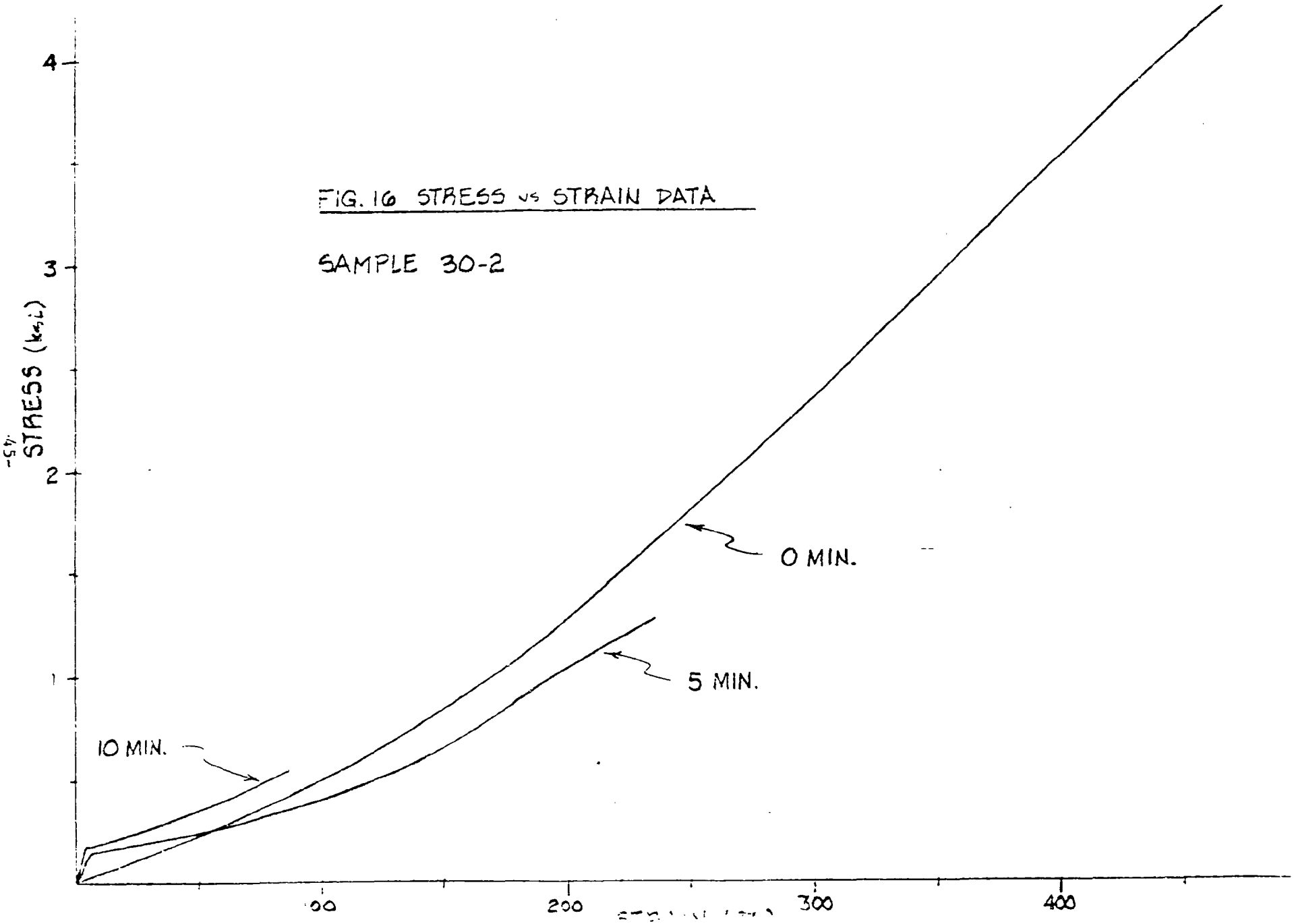
FIG. 16 STRESS vs STRAIN DATA
SAMPLE 30-2
STRESS (ksi)
4
3
2
1
0 MIN.
5 MIN.
10 MIN.
200
300
400

FIG. 17 STRESS vs STRAIN DATA

SAMPLE 30-3

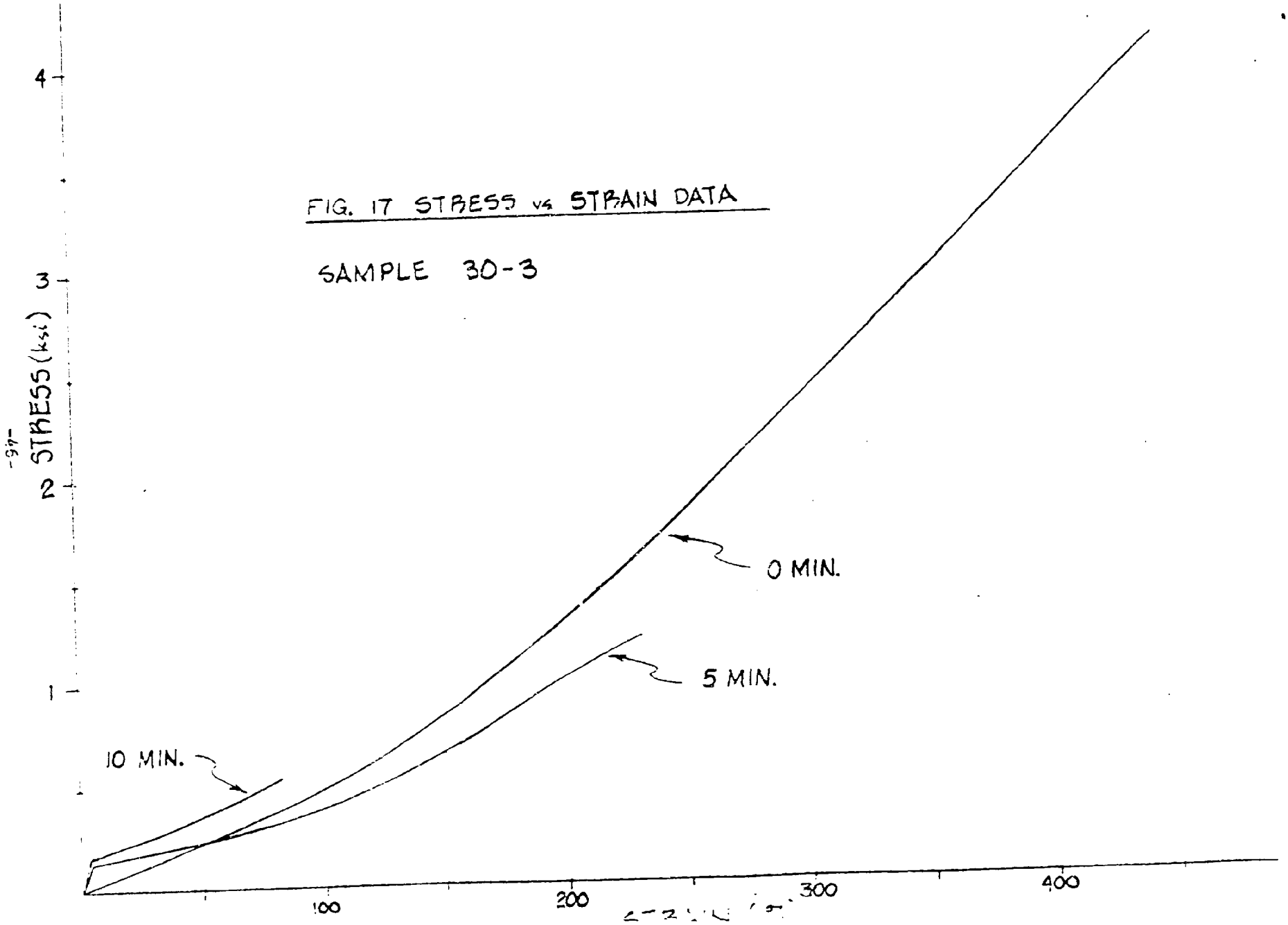

weight loss of a sample is measured continuously while its temperature is increased at a constant rate. This is done by placing the sample in a furnace while being suspended from one arm of a precision balance. The main use of TGA in application to polymers has been in studies of thermal decomposition and stability. A differential thermal analysis trace provides knowledge of the temperatures at which a thermal event occurs, and TGA tells whether the event is accompanied by weight loss.

A small initial weight loss, such as that from w to w_o, generally results from desorption of solvent. If it occurs near 100°C, this is usually assumed to be loss of water. In the example in the figure, extensive decomposition starts at T_1, with a weight loss $w_o - w_1$. Between T_2 and T_3 another stable phase exists, then further decomposition occurs.

DTA

Differential Thermal Analysis (DTA) is a technique for detecting the thermal effects accompanying physical or chemical changes in a reaction, by means of programmed heating or cooling.

A common DTA instrument includes the sample, a reference material, and a chamber contained in a heating block with an electrical heating element. Thermocouples placed in the centers of the sample and reference measure their temperature and also the temperature difference between them.

In a typical DTA experiment, the temperature of the heating block is programmed to increase linearly with time. The reference material is selected to be thermally inert except for slight changes in heat capacity with temperature. At the start of the experiment, the block, sample, and reference are all at the same temperature. As the block temperature rises, the temperatures registered by the thermocouples at the centers of the sample and reference rise more slowly due to the finite heat capacities of these material. Soon a steady state is reached, however, in which the

Figure 18

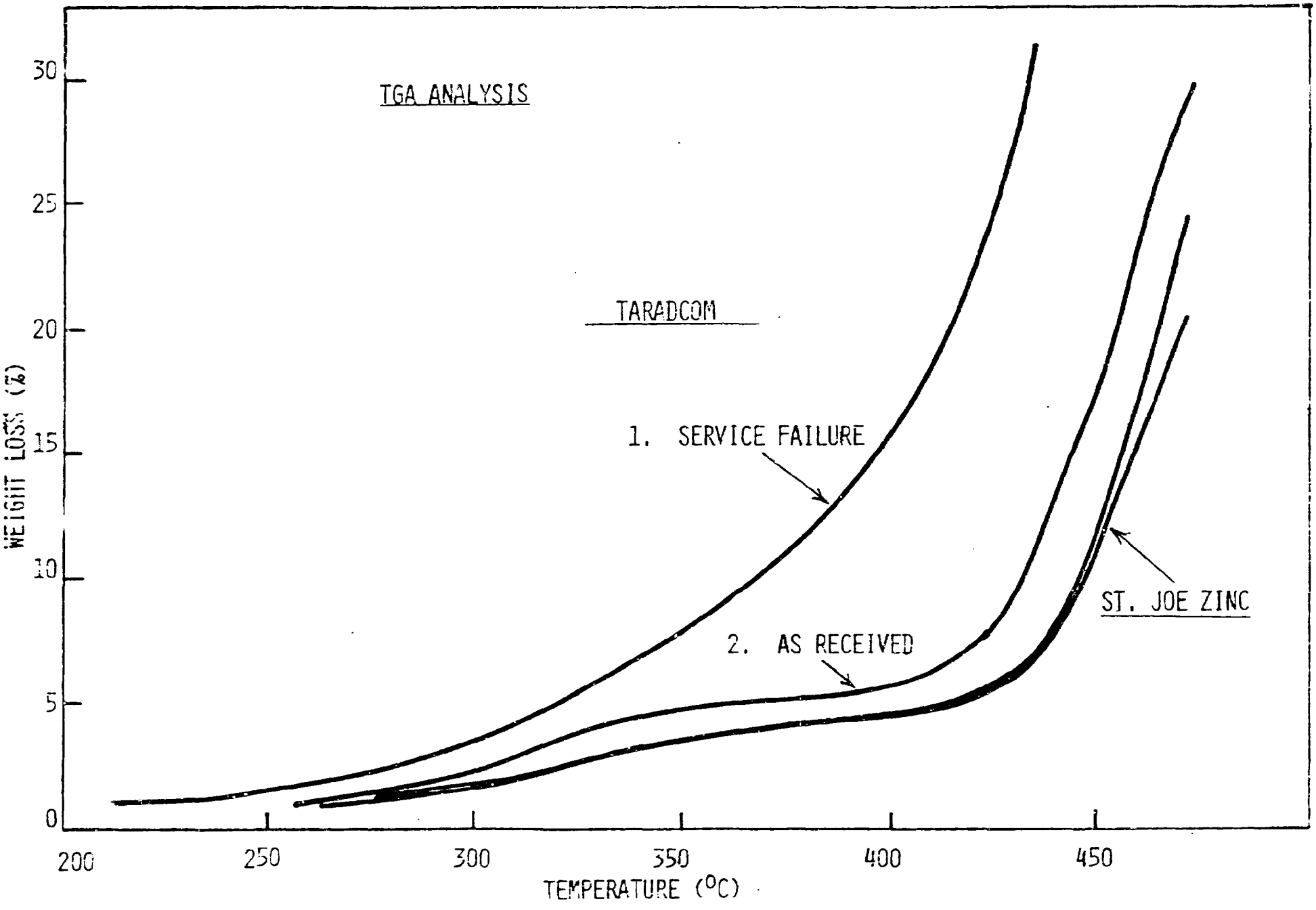
TGA ANALYSIS
TARADCOM
1. SERVICE FAILURE
2. AS RECEIVED
ST. JOE ZINC
WEIGHT LOSS (%)
0
5
10
15
20
25
30
200
250
300
350
400
450
TEMPERATURE (°C)

temperatures all rise uniformaly with time, and the temperature difference between the sample and reference is zero.

As the temperature reaches the glass-transition temperature of the sample, its heat capacity changes abruptly. The sample now absorbs more heat because of its higher heat capacity, and its temperature lagging behind the reference is increased. Its temperature therefore changes more slowly than that of the reference, with the results indicated in Fig. 19.

Similarily, other changes in the sample may occur as the block temperature is increased. For example, crystallization T_c and oxidation T_{ox} are exothermic reactions while melting and decomposition are endothermic.

Accelerated Decomposition

In trying to determine the cause of failure in rubber materials, unfailed material is sometimes put through an accelerated decomposition process in an attempt to obtain results that are similar to the original failed material. In the case of our tests, unfailed material was heated in an oven for various periods of time. The temperature of the oven was determined by looking at a TGA run of the failed material. Next, test runs were made and the temperature was adjusted to allow the sample to be heated a minimum of ten minutes without burning. The samples were then heated in the oven and tensile tested after they had cooled to see if they were approaching the characteristics of the failed material. Other tests such as DTA and TGA could also be done to compare the material.

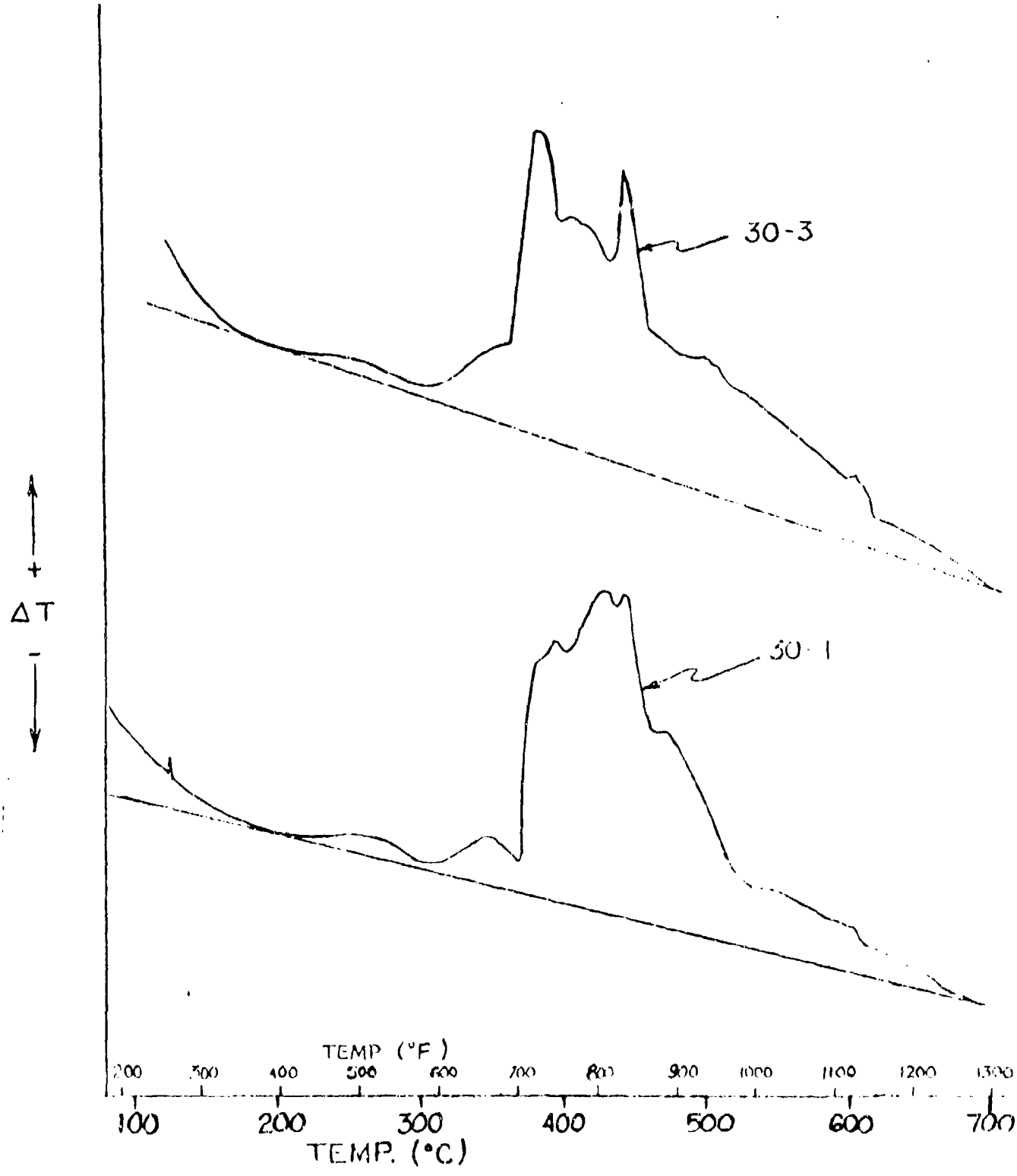

FIG. 19 DTA DATA

References

1. Wendlandt, W. Wm., Thermal Method of Analysis. 2nd ed. Wiley, New York, 1974.

2. Muilenberg, G. E., ed. Handbook of X-ray Photoelectron Spectroscopy. Eden Prairie, Minnesota: Perkin-Elmer Corporation, 1979.

3. Thorton, P. R., Scanning Electron Microscopy, Chapman & Hall Ltd., London, 1968.

4. Quantitative Scanning Electron Microscopy, ed. by D.B. Holt, M. D. Muir, P. R. Grant, and I. M. Boswarva, Academic Press, London, 1974.